

Title No. 111-S09

Crack Model for Steel Fiber-Reinforced Concrete Members Containing Conventional Reinforcement

by Jordon R. Deluce, Seong-Cheol Lee, and Frank J. Vecchio

This paper proposes a new model for the calculation of crack spacings and crack widths in steel fiber-reinforced concrete members containing conventional steel reinforcing bars (R/SFRC). The model considers the effects of various fiber and conventional reinforcement parameters. Predictions are compared against the test results of 17 plain reinforced concrete (RC) and 53 large-scale R/SFRC specimens subjected to uniaxial tension available in the literature. It is found that the proposed model predicts the crack spacings and widths of R/SFRC with reasonable accuracy and outperforms other steel fiber-reinforced concrete (SFRC) crack spacing models currently available. The model is expanded to include biaxial stress conditions to facilitate the analysis of elements such as SFRC panels subjected to shear. Here, too, the model is found to give sufficiently accurate predictions of the average crack conditions.

Keywords: biaxial; crack spacing; crack width; model; reinforced concrete; steel fiber; stress tension; uniaxial.

INTRODUCTION

The addition of discrete steel fibers of short length and small diameter to a concrete matrix greatly improves the tensile behavior of the material. When steel fibers are properly mixed into concrete, they are evenly dispersed through the bulk of the material and randomly oriented in three dimensions.^{1,2} When the material is subsequently subjected to tension and cracking, the plane of the crack will intercept some number of fibers. In SFRC exhibiting strain-softening behavior after cracking, as the crack widens, the steel fibers bridging the crack begin to elongate and transmit load across the crack. As the crack continues to widen, the force in a typical fiber continues to increase until the fiber's ultimate strength is reached and the fiber ruptures, causing an abrupt loss in load-carrying capacity; or until the shorter embedded length of the fiber overcomes its anchorage and begins to slip out, causing a gradual reduction in the load-carrying capacity.²⁻⁴ Alternatively, when a sufficiently large quantity of fibers of high aspect ratio is included in the concrete mix, the tensile behavior of the material can be strain-hardening in nature. In this case, a number of fibers bridging the initial crack allow for the transmission of a force larger than the initial cracking load, enabling multiple cracks to form in the concrete matrix, even if there are no continuous reinforcing bars present.^{5,6}

When SFRC is further reinforced by conventional reinforcing bars (R/SFRC), multiple cracks can form for strain-softening as well as strain-hardening SFRC. However, the multiple cracks which form in an R/SFRC member are narrower and more closely spaced than the cracks which form in a conventionally reinforced concrete (RC) member. When both fibers and conventional reinforcement bridge a crack, the tensile

force being transmitted across the crack is divided between the reinforcing bar and the fibers, resulting in a lower proportion of the load being resisted by the reinforcing bar than in an RC specimen under identical loading conditions. The ensuing lower stress and strain in the reinforcing bar results in a smaller local elongation at the crack location, and thus, smaller crack widths. In addition, as the steel fibers transmit tensile stress to the concrete matrix between cracks, the tensile stress in the concrete matrix increases more rapidly between the cracks in R/SFRC members than in RC members. This allows for the formation of more closely spaced cracks.⁷ Consequently, the beneficial effects derived from steel fibers go beyond improved cracking characteristics for R/SFRC; they also result in improved tension stiffening behavior and a larger post-yield load-carrying capacity relative to those observed in equivalent RC members.⁸

Given the interdependence of the cracking and tensile stress-strain behavior in R/SFRC, it is especially important in the analysis and design of such elements that the cracking characteristics be accurately modeled. Several researchers⁹⁻¹¹ investigated theoretically the tensile behavior of R/SFRC, but they focused on the tensile stress-crack width response rather than presenting a simple model for the average crack spacing. Although there are several simple cracking behavior models available in the literature,^{12,13} this investigation will show the need for improved procedures for calculating crack spacing and crack widths in R/SFRC members. A new model will be proposed for R/SFRC members containing end-hooked steel fibers, and its accuracy will be validated for both uniaxial and biaxial strain conditions.

RESEARCH SIGNIFICANCE

Although several formulations exist in the literature for modeling the crack characteristics of SFRC, none were found to predict the cracking behavior observed in a comprehensive test program conducted by Deluce and Vecchio¹⁴ with acceptable accuracy. This paper presents an improved formulation for calculating average crack spacings and maximum crack widths in SFRC specimens containing conventional reinforcement, under both uniaxial and biaxial stress conditions. Because the proposed model enables a rational evaluation of the tensile stresses attained by steel fibers for a given crack width,^{3,4} it can be implemented in various analysis models and programs¹⁵⁻¹⁹ and, thus, be

ACI Structural Journal, V. 111, No. 1, January-February 2014.
MS No. S-2012-022.R1, doi:10.14359.51686433, was received August 15, 2012, and reviewed under Institute publication policies. Copyright © 2014, American Concrete Institute. All rights reserved, including the making of copies unless permission is obtained from the copyright proprietors. Pertinent discussion including author's closure, if any, will be published ten months from this journal's date if the discussion is received within four months of the paper's print publication.

$$s_m = 50 + 0.25k_1k_2 \frac{d_b}{\rho_{s,eff}} \left(\frac{50}{l_f / d_f} \right) \quad (1)$$

where $50/(l_f/d_f) \leq 1$; k_1 is a factor meant to account for the bond characteristics of the reinforcing bars, taken as 0.8 for deformed reinforcing bars and 1.6 for smooth bars; k_2 is a factor accounting for strain gradient effects, calculated from $k_2 = (\varepsilon_1 + \varepsilon_2)/2\varepsilon_1$, where ε_1 and ε_2 are the largest and smallest tensile strains in the specimen, respectively; d_b and $\rho_{s,eff}$ are the conventional reinforcing bar diameter and reinforcement ratio, respectively; and l_f and d_f are the fiber length and diameter, respectively.

An alternative crack spacing model was proposed by Moffatt.¹² This formulation also modified the Eurocode 2²⁰ crack spacing model with a factor that reduces the crack spacing based on the ratio of the post-cracking residual stress of SFRC to the cracking stress

$$s_m = 50 + 0.25k_1k_2 \frac{d_b}{\rho_{s,eff}} \left(1 - \frac{f_{res}}{f_{cr}} \right) \quad (2)$$

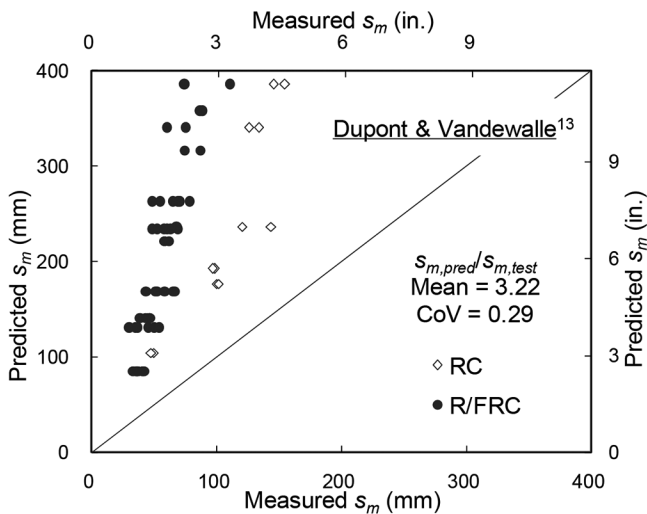
where f_{res} is the post-cracking residual concrete stress, and f_{cr} is the cracking stress of the concrete. Note that this formulation is only applicable to strain-softening materials.

There are some notable weaknesses in the above models. In the model proposed by Dupont and Vandewalle,¹³ the effect of the volumetric fiber content is not taken into the account; whether the fiber content is 0.1% or 5.0%, the prediction for average crack spacing remains constant. In the model proposed by Moffatt,¹² the determination of the residual tensile stress f_{res} is not straightforward without conducting tests on SFRC companion members with no conventional reinforcing bars. Therefore, the use of this formulation for analysis or design is not reliable given that the post-cracking residual stress is typically not known with confidence.

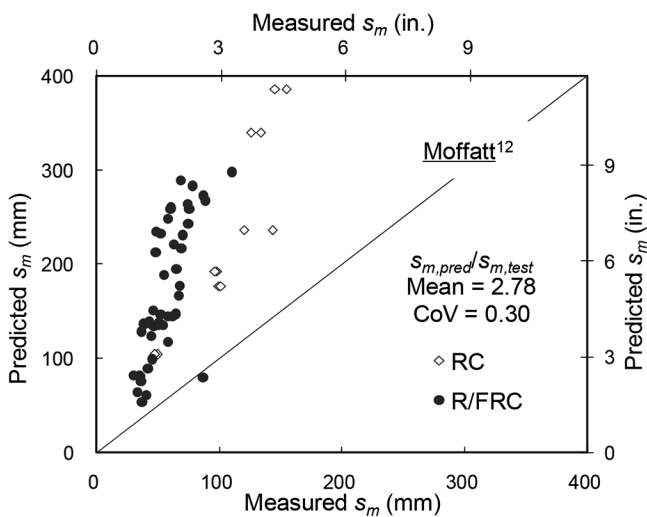
The average crack spacings predicted by Dupont and Vandewalle¹³ and Moffatt¹² were compared against those measured in the 47 R/SFRC tension tests conducted by Deluce and Vecchio.¹⁴ The test variables included fiber volumetric content, fiber length and aspect ratio, conventional reinforcement ratio, and steel reinforcing bar diameter, thus representing a comprehensive experimental investigation into the average crack spacing behavior in R/SFRC members. It is noted that the residual tensile stress of SFRC used in the Moffatt model was calculated by subtracting the yield force of the reinforcing bar from the total force of the member at the onset of plastic behavior, and dividing by the cross-sectional area of concrete. As presented in Fig. 1, it is evident that neither model predicts the average crack spacings adequately. The development of an improved formulation is required.

CRACKING BEHAVIOR MODEL AND VERIFICATION

It is generally accepted that the post-cracking tensile stress in an SFRC member is dependent on the crack widths,²⁻⁴ while the average tensile stress of the reinforcing bar is calculated from the average tensile strain of the bar.



(a)



(b)

Fig. 1—Average crack spacings in Deluce and Vecchio¹⁴ specimens predicted by previous formulations: (a) Dupont and Vandewalle¹³; and (b) Moffatt.¹²

useful for predictions of the structural behavior of R/SFRC members.

RE-EXAMINATION OF EXISTING CRACK SPACING MODELS

For evaluating the average crack spacing in R/SFRC members, several researchers have proposed simple formulations. The crack spacing model developed by Dupont and Vandewalle,¹³ for example, is one of the most frequently used SFRC crack spacing formulations available in literature. This model modifies the Eurocode 2²⁰ formulation for nonfibrous concrete by a factor that accounts for the reduction in average crack spacing caused by an increased fiber aspect ratio

Therefore, it is necessary to accurately model the cracking behavior of SFRC to be able to analyze and design R/SFRC structural members in which the tensile behavior of SFRC is considerable. In this regard, the relationship between the average crack width and average tensile strain is particularly important. In addition, the maximum crack width should also be known, not only for an evaluation of the serviceability of the R/SFRC structure, but also for the evaluation of ultimate capacity. This is because structural members under uniform loading fail at their weakest section, which typically corresponds with the location of the largest crack, as observed in the R/SFRC shear panel tests conducted by Susetyo.²¹ Thus, in this section, formulations for calculating average crack spacings and maximum crack widths in R/SFRC members will be described.

Uniaxial strain condition

Proposed crack spacing formulation—A formulation for the average stabilized crack spacing of steel fiber-reinforced concrete under uniaxial strain conditions has been developed and is presented herein. It is based on the CEB-FIP 1978²² crack spacing formulation, and modified to include parameters accounting for fiber content, length, and diameter. The formulation represents a fixed crack model in which only the stabilized crack spacing requires calculation.

To the CEB-FIP formulation the factor k_3 is introduced to account for the beneficial effects of steel fibers in regards to the influences from effective concrete cover and longitudinal reinforcing bar spacing. In addition, the reinforcement effectiveness parameter s_{mi} is modified to consider the tensile stress attained by steel fibers bridging cracks. The following formulation is thus proposed for describing the average stabilized crack spacing in R/SFRC members

$$s_m = 2 \left(c_a + \frac{s_b}{10} \right) k_3 + \frac{k_1 k_2}{s_{mi}} \quad (3)$$

where c_a is the effective concrete cover, which can be taken as 1.5 times the maximum aggregate size.

The parameter s_b is representative of the effective longitudinal bar spacing, estimated as follows

$$s_b = 0.5 \sqrt{\frac{\pi d_b^2}{\rho_{s,eff}}} \quad (4)$$

where d_b is the bar diameter, and $\rho_{s,eff}$ is the effective reinforcement ratio of conventional reinforcement. The variable s_b should not be taken as greater than $15d_b$.

To account for the influence of steel fibers bridging the cracks, by considering the number of fibers bridging a crack, the reinforcement effectiveness parameter s_{mi} is calculated from the following equation

$$s_{mi} = \frac{\rho_{s,eff}}{d_b} + k_f \frac{\alpha_f V_f}{d_f} \quad (5)$$

where α_f is the fiber orientation factor, which can be taken as 0.5 for the random three-dimensional (3-D) orientation of fibers in infinite elements. V_f is the fiber volume fraction, which is limited to a maximum value of 0.015 to consider the effect of fiber saturation on the tensile behavior of SFRC members. This fiber saturation effect was observed in direct tension tests of SFRC members conducted by Oh,²³ where the effect of increasing the fiber volume fraction of steel fibers beyond 0.015 caused only a minimal increase in tensile stress. The variable k_f is a factor accounting for fiber effectiveness due to the fiber aspect ratio, and is calculated as $k_f = l/50d_f \geq 1.0$ as presented in Dupont and Vandewalle.¹³

The parameter k_1 is a factor accounting for the bond characteristics of the reinforcing bars, having a value of 0.4 for deformed bars and 0.8 for plain bars and prestressing tendons. The parameter k_2 accounts for the strain conditions in the concrete member; its value is determined as $k_2 = 0.25(\varepsilon_1 + \varepsilon_2)/2\varepsilon_1$, where ε_1 and ε_2 are the largest and smallest tensile strains in the concrete, respectively. For a uniaxial strain condition, $k_2 = 0.25$. (Note: While k_1 and k_2 represent similar influences, as in the Eurocode 2²⁰ formulation, their numerical values differ.)

The parameter k_3 is a fiber content factor, calculated from the following equation

$$k_3 = 1 - \frac{\min(V_f, 0.015)}{0.015} \left(1 - \frac{1}{k_f} \right) \quad (6)$$

This factor modifies the effective cover and longitudinal bar spacing terms of Eq. (3). The influence of fiber saturation on tensile behavior is considered in Eq. (6) with the upper limitation of 0.015 for the fiber volume fraction, as was done in Eq. (5) when calculating the reinforcement effectiveness parameter s_{mi} . Essentially, for fiber contents between 0.0 and 1.5%, the value of k_3 is linearly interpolated between 1.0 and the value of 50 divided by the fiber aspect ratio.

This model captures the fact that as the fiber volume fraction or fiber aspect ratio increases, the average stabilized crack spacing decreases. When the fiber volume fraction is zero, the formulation reduces to a form similar to the CEB-FIP 1978²² average crack spacing formulation, but with the effective cover used in place of the actual concrete cover.

Proposed crack width formulation—To predict the serviceability behavior and ultimate capacity of R/SFRC members with accuracy, the ability to accurately model the crack widths of the material is important. Given the average stabilized crack spacing s_m , provided by the proposed formulation in Eq. (3), and the average tensile strain of a member $\varepsilon_{t,avg}$, an average crack width $w_{cr,avg}$ can be calculated

$$w_{cr,avg} = s_m \varepsilon_{t,avg} \quad (7)$$

However, the behavior of a member tends to be dominated by its weakest section, making the calculation of the maximum crack width necessary for the determination of the resistance of a section. For reinforced concrete members without fibers, it is frequently assumed that the maximum crack width is equal to about 1.7 times the average crack

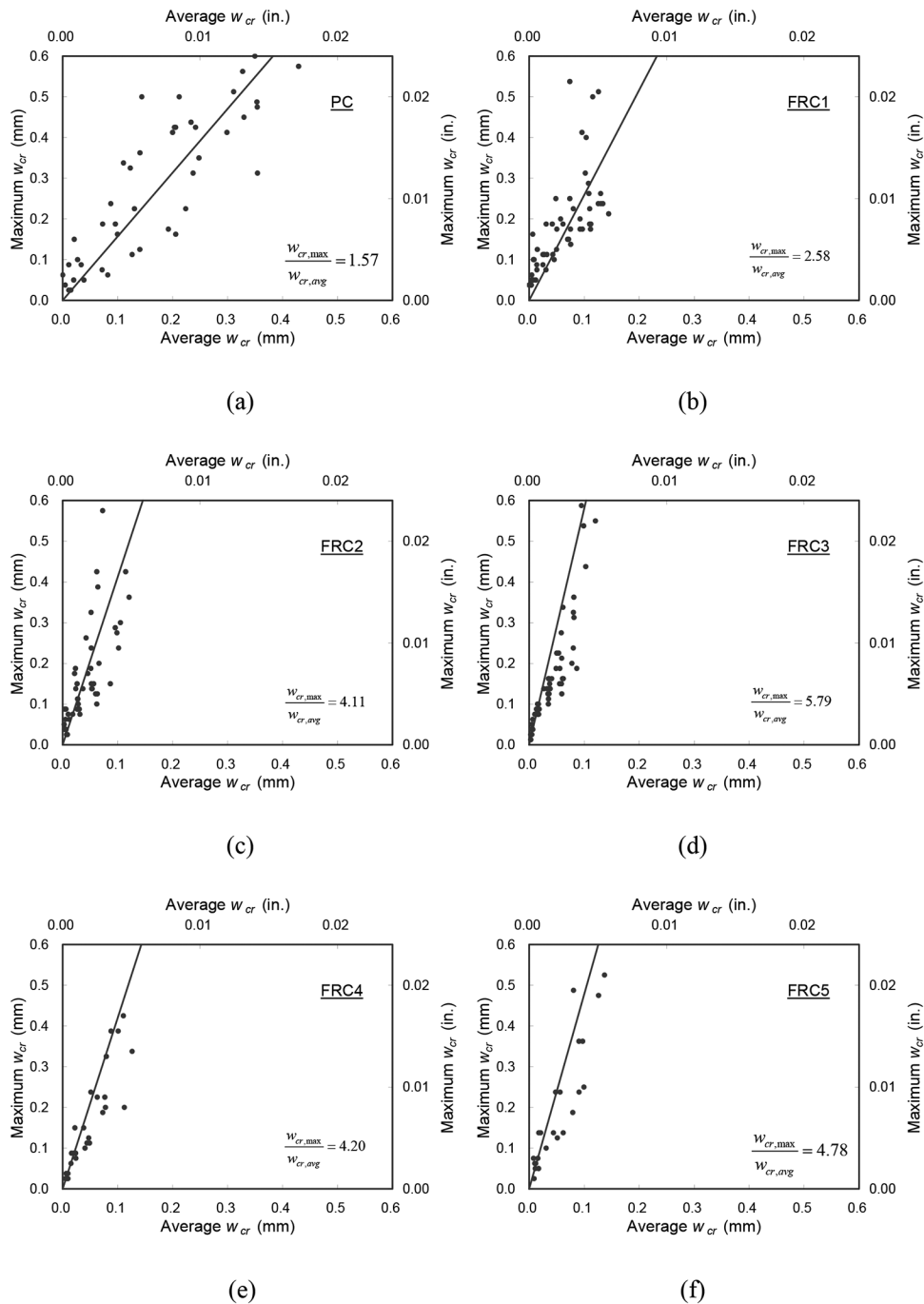


Fig. 2—Average and maximum crack widths in Deluce and Vecchio¹⁴ specimens: (a) PC; (b) FRC1; (c) FRC2; (d) FRC3; (e) FRC4; and (f) FRC5.

width²³; however, there is no equivalent relationship for R/SFRC members available in the literature. To develop this relationship, the average and maximum crack widths of the specimens tested by Deluce and Vecchio¹⁴ were compared (Fig. 2). It can be seen that the typical ratio of maximum to average crack widths was 1.57 for the nonfibrous specimens, which is close to the generally accepted value of 1.7. However, it can also be seen that for R/SFRC, as the fiber volume fraction or aspect ratio increases, so too does the ratio of maximum to average crack width for a given strain. By introducing a fiber effectiveness parameter consisting of the product of the fiber volume fraction and aspect ratio,

the maximum crack width $w_{cr,max}$ can be calculated from the average crack width in Eq. (7) as follows

$$w_{cr,max} = \left(1.7 + 3.4 \frac{V_f l_f}{d_f} \right) w_{cr,avg} \quad (8)$$

This function is only valid for strains less than the yielding strain; Eq. (8) is not valid for post-yield behavior because deformations begin to localize at one or more cracks. Figure 3 plots the ratio of maximum to average crack width as a function of the fiber effectiveness parameter. The data points shown in this figure are evaluated from the average

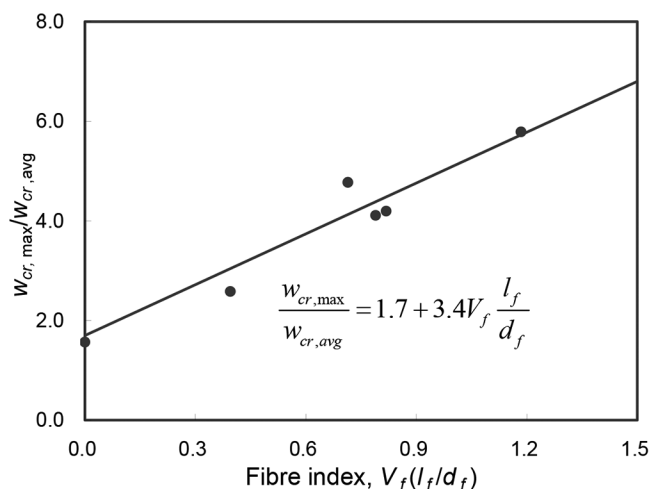


Fig. 3—Effect of fiber index on ratio of maximum to average crack widths.

ratios of maximum to mean crack widths for each test series examined in Fig. 2. It can be seen that the values of the ratio generated by Eq. (8) are in close agreement to those observed experimentally.

Validation of proposed uniaxial cracking behavior formulations—To investigate the accuracy of the proposed model, it was used to calculate the average stabilized crack spacings of the 12 RC and 47 R/SFRC specimens tested at the University of Toronto.¹⁴ The details of the test program were presented by Deluce.²⁴ Plots comparing the predicted stabilized crack spacings to those experimentally are shown in Fig. 4(a), and the specimen details are given in Table 1. It can be seen from the figure and table that the proposed crack spacing formulation provides reasonably accurate predictions of the observed crack spacings of both RC and R/SFRC specimens under uniaxial strain conditions.

In addition to those for specimens tested by Deluce and Vecchio,¹⁴ the predictions of the proposed average crack spacing model were compared with the test results of several uniaxial tension tests of R/SFRC specimens obtained by Abrishami and Mitchell,²⁵ Noghabai,²⁶ and Bischoff.⁸ Abrishami and Mitchell²⁵ tested two RC and two R/SFRC specimens, 90 x 170 mm (3.54 x 6.69 in.) by 1500 mm (59.1 in.) in length, containing a 15M reinforcing bar. Noghabai²⁶ tested one RC and two R/SFRC specimens, 80 x 80 mm (3.15 x 3.15 in.) by 960 mm (37.8 in.) in length, containing a 15M reinforcing bar. Bischoff⁸ tested two RC and two R/SFRC specimens; the specimens were 1100 mm (43.3 in.) long, and 100 x 100 mm (3.94 x 3.94 in.) in cross section. One nonfibrous and one R/SFRC specimen contained a 15M reinforcing bar, while the other two specimens contained a 20M reinforcing bar. Table 2 presents the geometric and material parameters of the relevant specimens tested in the three experimental programs and compares the stabilized crack spacings predicted by the proposed model to the values reported by the authors. Figure 4(b) plots the predicted crack spacings against those experimentally observed. It must be noted that, for Abrishami and Mitchell²⁵ and Noghabai,²⁶ the crack spacings were estimated from diagrams of crack patterns and low-resolution photographs

of the tested specimens, respectively. It can be seen that the proposed average crack spacing model predicts the observed values with reasonable accuracy.

Figure 5 plots the predictions of maximum crack widths against those experimentally observed by Deluce.²⁴ (Note that because none of the other authors reported crack widths, the comparison was conducted only for the test results presented by Deluce and Vecchio.¹⁴) It can be seen from the figure that the proposed crack width model predicts the experimentally observed maximum crack widths with an acceptable accuracy; however, as should be expected, the results show significant scatter.

Biaxial strain condition

Proposed crack spacing formulation—Many types of structural members are subjected to biaxial strain conditions, most notably when axial and flexural actions are accompanied by shear or torsion. Thus, it is essential that the uniaxial crack spacing models be extended to include biaxial strain conditions. Because steel fibers contribute to the principal tensile stress in R/SFRC members, the parameters s_b and s_{mi} in Eq. (4) and (5) should be evaluated with respect to the principal tensile axis. These values are then entered into the crack spacing formulation proposed in Eq. (3).

The effective longitudinal bar spacing in the principal tensile direction, s_{b1} , can be calculated as follows

$$s_{b1} = \frac{1}{\sqrt{\sum_i \frac{4 \rho_{s,i}}{\pi d_{b,i}^2} \cos^4 \theta_i}} \quad (9)$$

where i represents a layer of reinforcement in a given direction; $\rho_{s,i}$, $d_{b,i}$, and θ_i are the reinforcement ratio, bar diameter, and orientation of the i reinforcement, respectively, with the angle measured from the principal tensile strain direction.

In a manner similar to that for ordinary reinforced concrete structures,²⁷ s_{mi} for a biaxial strain condition can be calculated as follows

$$s_{mi} = \sum_i \frac{\rho_{s,i}}{d_{b,i}} \cos^2 \theta_i + k_f \frac{\alpha_f V_f}{d_f} \quad (10)$$

These parameters can then be substituted into the crack spacing formulation of Eq. (3), and this crack spacing can be used to determine the average and maximum crack widths in accordance with Eq. (7) and (8).

Validation of proposed biaxial cracking behavior formulations—To verify the proposed average crack spacing model for biaxial strain conditions, the model's predictions were compared with test results reported by Susetyo,²¹ wherein two RC and eight R/SFRC panels were tested under pure shear. Each panel was 870 x 870 x 70 mm (34.25 x 34.25 x 2.76 in.). The nominal concrete strength was 50 MPa (7250 psi) or 80 MPa (11600 psi), and the amounts of conventional and steel fiber reinforcement were varied (refer to Table 3). In these tests, the first crack occurred when the principal angle was approximately equal

Table 1—Average crack spacings in specimens tested by Deluce and Vecchio¹⁴

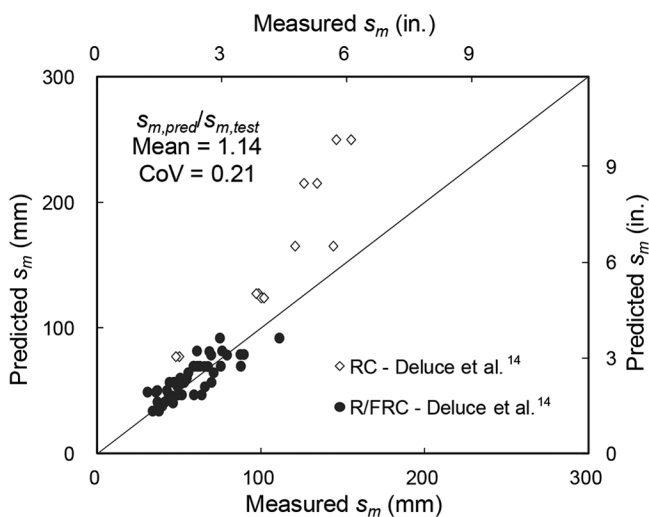
Specimen	f'_c , MPa	ρ_s , %	d_b , mm	V_f , %	l_p , mm	d_p , mm	$s_{m,test}$, mm	$s_{m,pred}$, mm	$s_{m,pred}/s_{m,test}$		
PC-50/10	91.8	4.00	11.3	0.0	—	—	50	77	1.55		
							48		1.61		
PC-80/10	91.7	1.56	11.3						98	127	1.29
							97	1.31			
PC-100/20	92.2	3.00	19.5						100	124	1.24
							102	1.22			
PC-150/20	92.6	1.33	19.5			134	215	1.60			
				126	1.71						
PC-150/30	91.9	3.11	29.9			121	165	1.37			
				144	1.15						
PC-200/30	95.0 95.6	1.75	29.9			155	250	1.61			
				146	1.71						
FRC1-50/10	87.2 93.3	4.00	11.3	0.5	30	0.38	42	50	1.18		
							37		1.37		
FRC1-80/10	79.2	1.56	11.3						46	57	1.22
							47	1.20			
FRC1-100/20	91.4	3.00	19.5						55	60	1.10
							51	1.19			
FRC1-150/20	81.8	1.33	19.5			61	70	1.14			
				59	1.19						
FRC1-150/30	55.8	3.11	29.9			65	69	1.06			
				67	1.03						
FRC1-200/30	62.1 69.4	1.75	29.9			79	79	0.99			
				69	1.13						
FRC2-50/10	57.8	4.00	11.3	1.0	30	0.38	41	41	1.00		
							37		1.12		
FRC2-80/10	57.5	1.56	11.3						45	46	1.02
							44	1.06			
FRC2-100/20	58.1	3.00	19.5						31	49	1.60
							36	1.37			
FRC2-150/20	45.2	1.33	19.5			70	57	0.82			
				53	1.07						
FRC2-150/30	55.0	3.11	29.9			53	57	1.07			
				44	1.29						
FRC2-200/30	59.4 63.4	1.75	29.9			55	64	1.16			
				61	0.91						
FRC3-50/10	52.0 52.6	4.00	11.3	1.5	30	0.38	38	34	0.90		
							34		1.01		
FRC3-80/10	52.6 53.2	1.56	11.3						40	38	0.96
							39	0.97			
FRC3-100/20	62.0	3.00	19.5						46	40	0.88
							37	1.09			
FRC3-150/20	62.0	1.33	19.5			64	47	0.74			
				49	0.95						
FRC3-150/30	46.0	3.11	29.9			59	47	0.80			
				52	0.91						
FRC3-200/30	63.1	1.75	29.9			49	53	1.09			
				66	0.81						
FRC4-150/20	52.8	1.33	19.5	1.5	30	0.55	88	70	0.80		
							75		0.93		
FRC4-150/30	32.5	3.11	29.9						62	70	1.11
				59	1.18						
FRC4-200/30	46.5	1.75	29.9			89	79	0.88			
				87	0.90						
FRC5-150/20	78.8	1.33	19.5	1.5	50	1.05	76	82	1.07		
							61		1.34		
FRC5-150/30	77.0	3.11	29.9						68	81	1.19
				85	0.83						
FRC5-200/30	70.3	1.75	29.9			75	92	1.23			
Average									1.14		
Coefficient of variation									0.21		

Notes: 1 mm = 0.0394 in.; 1 MPa = 145 psi.

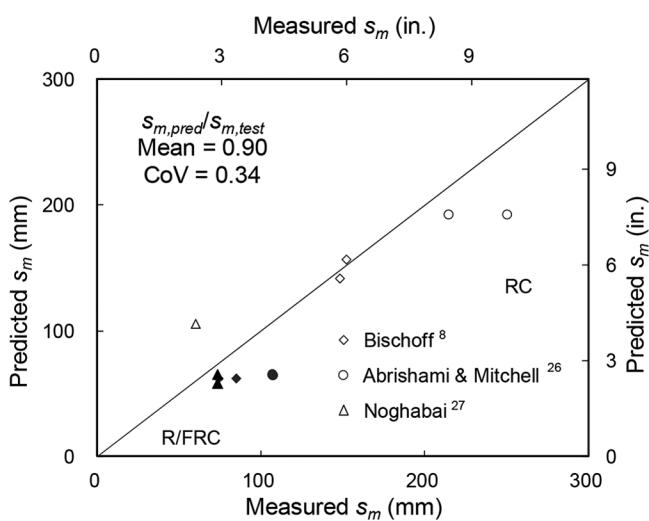
Table 2—Average crack spacings in specimens tested by other researchers^{8,25,26}

Research group	Specimen	f'_c , MPa	ρ_s , %	d_p , mm	V_f , %	l_f , mm	d_f , mm	$s_{m,test}$, mm	$s_{m,pred}$, mm	$s_{m,pred}/s_{m,test}$
Bischoff ⁸	RC-15M	62.8	2.00	16.0	0.0	—	—	152	157	1.03
	FRC-15M	62.4	2.00	16.0	0.8	50	0.5	85	62	0.73
	RC-20M	62.8	3.00	19.5	0.0	—	—	148	142	0.96
	FRC-20M	62.4	3.00	19.5	0.8	50	0.5	74	62	0.84
Abrishami and Mitchell ²⁵	CO	34.9	1.24	16.0	0.0	—	—	250	193	0.77
	HCO	90.0	1.24	16.0	0.0	—	—	214	193	0.90
	FCO	30.8	1.24	16.0	1.0	30	0.5	107	65	0.61
	FHCO	74.6	1.24	16.0	1.0	30	0.5	107	65	0.61
Noghabai ²⁶	HSC-REF	97.3	3.14	16.0	0.0	—	—	60	106	1.77
	HSC-S30/0.6	103.7	3.14	16.0	1.0	30	0.6	74	65	0.88
	HSC-S6/0.15	105.8	3.14	16.0	1.0	6	0.15	74	58	0.78
Average										0.90
Coefficient of variation										0.34

Notes: 1 mm = 0.0394 in.; 1 MPa = 145 psi.



(a)



(b)

Fig. 4—Average crack spacings calculated from proposed model compared to values measured by: (a) Deluce and Vecchio¹⁴; and (b) other researchers.^{8,25,26}

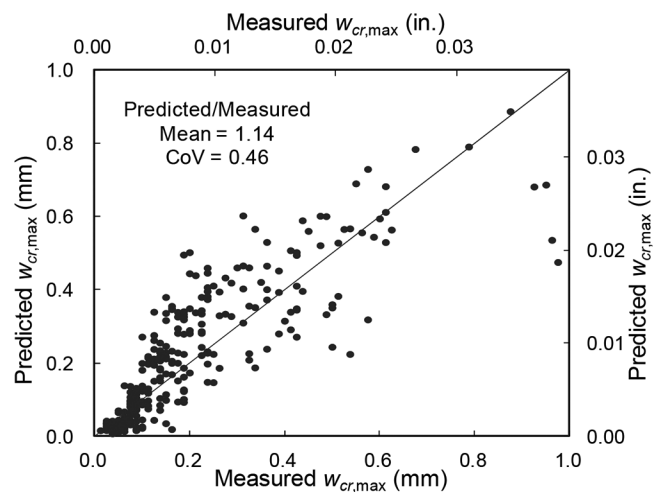


Fig. 5—Maximum crack widths calculated from proposed model compared to values measured by Deluce and Vecchio.¹⁴

to 45 degrees. As the magnitude of the shear force increased, the principal angle also increased. At the onset of stabilized cracking for each panel, the principal directions had typically rotated to approximately 60 degrees. Figure 6 shows the crack patterns of RC and R/SFRC panels at failure. As presented in the figure, the average crack spacing in the R/SFRC panel (C1F2V3) is much smaller than those in the RC panel (C1C-R) although the R/SFRC panel did not have any of the transverse reinforcing bars that were present in the RC panel. The average crack spacings measured during the stabilized cracking phase are presented in Table 3, along with the average crack spacing calculated from the proposed model for biaxial strain conditions. From Table 3 and Fig. 7, it can be concluded that the average crack spacing in a biaxial strain condition can be calculated with reasonable accuracy by the proposed model.

CONCLUSIONS

To correctly calculate the structural behavior of R/SFRC members, it is important to be able to accurately estimate the average crack conditions that they will experience. This is because the tensile stress attained by steel fibers is directly

Table 3—Average stabilized crack spacings in R/SFRC shear panels tested by Susetyo²¹

Specimen	f'_c , MPa	$\rho_{s,x}$, %	$d_{b,x}$, mm	$\rho_{s,y}$, %	$d_{b,y}$, mm	V_f , %	l_f , mm	d_f , mm	$s_{m,test}$, mm	$s_{m,pred}$, mm	$s_{m,pred}/s_{m,test}$
C1C-R	65.7	3.31	8.0	0.42	4.01	0.0	—	—	57	98	1.72
C1F1V1	51.4	3.31	8.0	—	—	0.5	30	0.38	114	67	0.58
C1F1V2	53.4	3.31	8.0	—	—	1.0	30	0.38	55	53	0.97
C1F1V3	49.7	3.31	8.0	—	—	1.5	30	0.38	57	43	0.75
C1F2V3	59.7	3.31	8.0	—	—	1.5	35	0.55	38	42	1.10
C1F3V3	45.5	3.31	8.0	—	—	1.5	50	0.62	57	54	0.94
C2C-R	90.5	3.31	8.0	0.42	4.01	0.0	—	—	66	98	1.48
C2F1V3	78.8	3.31	8.0	—	—	1.5	30	0.38	36	43	1.19
C2F2V3	76.5	3.31	8.0	—	—	1.5	35	0.55	47	42	0.90
C2F3V3	62.0	3.31	8.0	—	—	1.5	50	0.62	41	54	1.32
Average											1.09
Coefficient of variation											0.30

Notes: 1 mm = 0.0394 in.; 1 MPa = 145 psi.

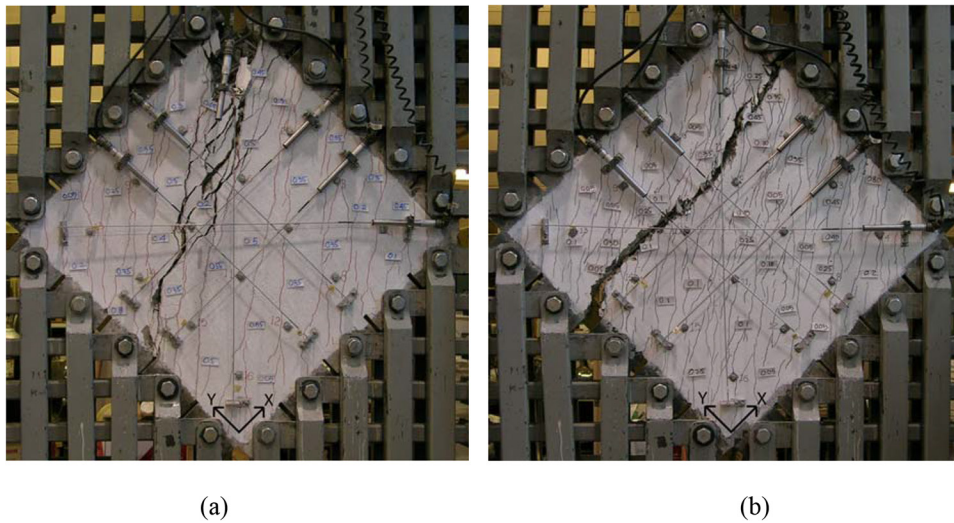


Fig. 6—Crack patterns at failure in R/SFRC shear panels tested by Susetyo²¹: (a) C1C-R; and (b) C1F2V3.

dependent on crack width while the tensile stress of conventional reinforcing bars is calculated from the average tensile strain. Consequently, a reliable crack spacing model is required to provide the relationship between average tensile strains and crack widths. However, from an examination of test results involving R/SFRC members subjected to tension, it was discovered that the previously developed models available in literature do not provide accurate predictions of the average crack spacings observed.

To address this deficiency, a new crack spacing model was developed to account for parameters such as reinforcement ratio, reinforcing bar size, fiber content, fiber length, and fiber diameter. The proposed model performed significantly better than the existing models. In addition, because the relationship between average crack widths and maximum crack widths can be assumed to be linear, an empirical formula was proposed to calculate the average to maximum crack width conversion factor as a function of fiber volume content and aspect ratio. This allowed the calculation of the maximum

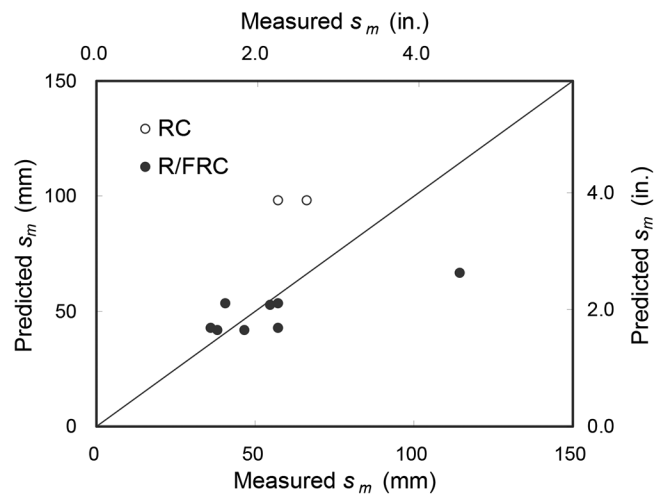


Fig. 7—Comparison of calculated and measured average crack spacings in R/SFRC shear panels tested by Susetyo.²¹

crack width from the average crack width predicted by the proposed average crack spacing model. Although a degree of scatter was observed, the proposed relationship was found to predict the maximum crack widths with acceptable accuracy.

The proposed formulation for average crack spacing was extended to biaxial strain conditions. Through comparisons with the test results of the R/SFRC panels subjected to pure shear, it was shown that the proposed model predicts the average crack spacing in R/SFRC panels under biaxial strain conditions with acceptable accuracy.

The proposed models are of a form that can be easily implemented in analysis models and programs so that they can be useful in the prediction of the structural behavior of R/SFRC members with end-hooked steel fibers. Further study is recommended for determining the applicability of the model to other types of fibers such as straight fibers, crimped fibers, and synthetic fibers.

ACKNOWLEDGMENTS

This project was funded by the National Sciences and Engineering Research Council of Canada (NSERC) under the Engage Grant program, with Bekaert Canada Ltd. being the industrial collaborator. The authors would like to gratefully acknowledge the funding provided by NSERC. In addition, generous material donations were made by N.V. Bekaert S.A., Sika Canada Inc., Holcim Canada Inc., Dufferin Aggregates, and BASF Canada. This project was part of a collaborative program undertaken jointly with the University of Brescia, and their participation is also gratefully acknowledged.

AUTHOR BIOS

ACI member Jordon R. Deluce is currently employed at Morrison Hershfield Ltd. in Vancouver, BC, Canada. He received his MASc from the Department of Civil Engineering at the University of Toronto, Toronto, ON, Canada, in 2011. His research interests include nonlinear analysis and performance assessment of reinforced concrete structures, shear effects in reinforced concrete, and the tensile behavior and cracking characteristics of steel fiber-reinforced concrete.

ACI member Seong-Cheol Lee is an Assistant Professor at KEPCO International Graduate School (KINGS), South Korea, and was a Postdoctoral Researcher in the Department of Civil Engineering at the University of Toronto. He received his PhD from Seoul National University, Seoul, South Korea, in 2007. His research interests include the shear behavior of concrete structures, the analysis of prestressed concrete structures, and fiber-reinforced concrete members.

Frank J. Vecchio, F.ACI, is a Professor of civil engineering at the University of Toronto. He is a member of Joint ACI-ASCE Committees 441, Reinforced Concrete Columns, and 447, Finite Element Analysis of Concrete Structures. He received the ACI Structural Research Award in 1998, the ACI Structural Engineering Award in 1999, and the Wason Medal for Most Meritorious Paper in 2011. His research interests include advanced constitutive modeling, assessment and rehabilitation of concrete structures, and response under extreme load conditions.

NOTATION

c_a	=	effective concrete cover
d_b	=	diameter of conventional reinforcing bar
$d_{b,i}$	=	diameter of conventional reinforcing bar oriented in i-direction
$d_{b,x}$	=	diameter of conventional reinforcing bar oriented in x-direction
$d_{b,y}$	=	diameter of conventional reinforcing bar oriented in y-direction
d_f	=	diameter of steel fiber
f'_c	=	peak concrete compression cylinder strength
f_{cr}	=	concrete cracking stress
f_{res}	=	post-cracking residual tensile stress
i	=	given reinforcement direction
k_1	=	factor accounting for bond characteristics of conventional reinforcing bars

k_2	=	factor accounting for strain gradient
k_3	=	factor accounting for fiber content
k_f	=	factor accounting for fiber aspect ratio
l_f	=	fiber length
s_b	=	effective longitudinal bar spacing
s_{b1}	=	effective longitudinal bar spacing in principal tensile direction
s_m	=	mean stabilized crack spacing
s_{mi}	=	reinforcement effectiveness parameter in principal tensile direction
$s_{m,pred}$	=	predicted stabilized mean crack spacing
$s_{m,test}$	=	experimentally observed stabilized mean crack spacing
V_f	=	volumetric fiber content
w_{cr}	=	crack width
$w_{cr,avg}$	=	average crack width
$w_{cr,max}$	=	maximum crack width
α_f	=	fiber orientation factor
ϵ_1	=	largest tensile strain through specimen cross section
ϵ_2	=	smallest tensile strain through specimen cross section
ϵ	=	average tensile strain
$\theta_i^{t,avg}$	=	angle between given reinforcement axis and principal tensile direction
ρ_s	=	reinforcement ratio for conventional reinforcement
$\rho_{s,eff}$	=	effective reinforcement ratio
$\rho_{s,i}$	=	reinforcement ratio for conventional reinforcement in i-direction
$\rho_{s,x}$	=	reinforcement ratio for conventional reinforcement in x-direction
$\rho_{s,y}$	=	reinforcement ratio for conventional reinforcement in y-direction

REFERENCES

- Naaman, A. E., "A Statistical Theory of Strength for Fiber Reinforced Concrete," PhD thesis, Department of Civil Engineering, Massachusetts Institute of Technology, Cambridge, MA, 1972, 196 pp.
- Voo, J. Y. L., and Foster, S. J., "Variable Engagement Model for Fibre Reinforced Concrete in Tension," *UNICIV Report No. R-420*, The University of New South Wales, Sydney, Australia, June 2003, pp. 1-86.
- Lee, S.-C.; Cho, J.-Y.; and Vecchio, F. J., "Diverse Embedment Model for Fiber-Reinforced Concrete in Tension: Model Development," *ACI Materials Journal*, V. 108, No. 5, Sept.-Oct. 2011, pp. 516-525.
- Lee, S.-C.; Cho, J.-Y.; and Vecchio, F. J., "Diverse Embedment Model for Fiber-Reinforced Concrete in Tension: Model Verification," *ACI Materials Journal*, V. 108, No. 5, Sept.-Oct. 2011, pp. 526-535.
- Chao, S. H.; Naaman, A. E.; and Parra-Montesinos, G. J., "Bond Behavior of Reinforcing Bars in Tensile Strain-Hardening Fiber-Reinforced Cement Composites," *ACI Structural Journal*, V. 106, No. 6, Nov.-Dec. 2009, pp. 897-906.
- Naaman, A. E., "Tensile Strain-Hardening FRC Composites: Historical Evolution Since the 1960s," *Proceedings of International Workshop on Advanced Construction Materials*, Springer-Verlag, Berlin, Germany, 2007, pp. 181-202.
- Lee, S.-C.; Cho, J.-Y.; and Vecchio, F. J., "Tension Stiffening Model for Steel Fiber-Reinforced Concrete Containing Conventional Reinforcement," *ACI Structural Journal*, V. 110, No. 4, July-Aug. 2013, pp. 639-648.
- Bischoff, P. H., "Tension Stiffening and Cracking of Steel Fiber-Reinforced Concrete," *Journal of Materials in Civil Engineering*, ASCE, V. 15, No. 2, Apr. 2003, pp. 174-182.
- Stang, H., and Aarre, T., "Evaluation of Crack Width in FRC with Conventional Reinforcement," *Cement and Concrete Composites*, V. 14, No. 2, Feb. 1992, pp. 143-154.
- Stang, H.; Li, V. C.; and Krenchel, H., "Design and Structural Applications of Stress-Crack Width Relations in Fibre Reinforced Concrete," *Materials and Structures*, V. 28, No. 4, May 1995, pp. 210-219.
- Chiaia, B.; Fantilli, A. P.; and Vallini, P., "Evaluation of Crack Width in FRC Structures and Application to Tunnel Linings," *Materials and Structures*, V. 42, No. 3, Apr. 2009, pp. 339-351.
- Moffatt, K., "Analyse de Dalles de Pont avec Armature Réduite et Béton de Fibres Métalliques," MScA thesis, École Polytechnique de Montréal, Montreal, QC, Canada, 2001, 248 pp.
- Dupont, D., and Vandewalle, L., "Calculation of Crack Widths with the σ - ϵ Method," *Test and Design Methods for Steel Fibre Reinforced Concrete: Background and Experiences—Proceedings of the RILEM TC162-TDF Workshop*, RILEM Technical Committee 162-TDF, Bochum, Germany, 2003, pp. 119-144.
- Deluce, J. R., and Vecchio, F. J., "Cracking Behavior of Steel Fiber-Reinforced Concrete Members Containing Conventional Reinforcement," *ACI Structural Journal*, V. 110, No. 3, May-June 2013, pp. 481-490.
- Vecchio, F. J., and Collins, M. P., "The Modified Compression Field Theory for Reinforced Concrete Elements Subjected to Shear," *ACI Journal*, V. 83, No. 2, Mar.-Apr. 1986, pp. 219-231.

16. Bentz, E. C., "Sectional Analysis of Reinforced Concrete Members," doctorate thesis, Department of Civil Engineering, University of Toronto, Toronto, ON, Canada, 2000, 184 pp.
17. Vecchio, F. J., "Disturbed Stress Field Model for Reinforced Concrete: Formulation," *Journal of Structural Engineering*, ASCE, V. 126, No. 9, Sept. 2000, pp. 1070-1077.
18. Vecchio, F. J., "Disturbed Stress Field Model for Reinforced Concrete: Implementation," *Journal of Structural Engineering*, ASCE, V. 127, No. 1, Jan. 2001, pp. 12-20.
19. Wong, P. S., and Vecchio, F. J., "VecTor2 & FormWorks User's Manual," *Publication No. 2002-02*, Department of Civil Engineering, University of Toronto, Toronto, ON, Canada, Aug. 2002, 214 pp.
20. EN 1992-1-1:2004, "Eurocode 2: Design of Concrete Structures – Part 1-1: General Rules and Rules for Buildings," 2004, 226 pp.
21. Susetyo, J., "Fibre Reinforcement for Shrinkage Crack Control in Prestressed, Precast Segmental Bridges," PhD dissertation, University of Toronto, Toronto, ON, Canada, www.civ.utoronto.ca/vector/theses.html, 2009, 532 pp.
22. Comité Euro International du Béton (CEB/FIP), "Model Code for Concrete Structures," *CEB-FIP International Recommendations*, third edition, Paris, France, 1978, 348 pp.
23. Collins, M. P., and Mitchell, D., *Prestressed Concrete Structures*, Prentice Hall, Englewood Cliffs, NJ, 1993, 766 pp.
24. Deluce, J., "Cracking Behaviour of Steel Fibre Reinforced Concrete Containing Conventional Steel Reinforcement," MSc thesis, University of Toronto, Toronto, ON, Canada, www.civ.utoronto.ca/vector/theses.html, 2011, 506 pp.
25. Abrishami, H. H., and Mitchell, D., "Influence of Steel Fibers on Tension Stiffening," *ACI Structural Journal*, V. 94, No. 6, Nov.-Dec. 1997, pp. 769-776.
26. Noghabai, K., "Behavior of Tie Elements of Plain and Fibrous Concrete and Varying Cross Sections," *ACI Structural Journal*, V. 97, No. 2, Mar.-Apr. 2000, pp. 277-285.
27. Bentz, E. C., "Explaining the Riddle of Tension Stiffening Models for Shear Panel Experiments," *Journal of Structural Engineering*, ASCE, V. 131, No. 9, Sept. 2005, pp. 1422-1425.
28. Oh, J.-H., "Uniaxial Behavior of Steel Fiber Reinforced Concrete," master's thesis, Seoul National University, Seoul, South Korea, 2011, 122 pp. (in Korean)